Forest Chemicals Review
www.forestchemicalsreview.com
ISSN: 1520-0191
Sept-Oct 2021 Page No. 1243-1252
Article History: Received: 10 August 2021, Revised: 25 August 2021, Accepted: 05 September 2021, Publication: 31 October 2021

Application of Symmetry Properties on the Hybrid Method in Time Domain

Yu Guo[1], Wei Wang[2], Ting Chen[3], Xiaowang Tong[4*]
[1]Merchant Marine College, Shanghai Maritime University, Shanghai, China
[2]Erection Department, Jiangnan Shipbuilding (group) co. LTD, Shanghai, China
[3]China Classification Society Shanghai Branch, China Classification Society, Shanghai, China
[4]Jiangnan Institute of Technology, Jiangnan Shipbuilding (group) co. LTD, Shanghai, China
*Corresponding Author.

Abstract:

Compared with the frequency-domain method, the time-domain method requires more storage space and computation in the hydrodynamic calculation of ships and marine structures. Establish a hybrid boundary integral equation coupled with Rankine source method and time-domain Green function method, solutions on the control surface were satisfied the far-field radiation condition with Rankine source method. According to the hybrid boundary model, the parts of time-domain Green function were only contained on the control surface. So this paper choose a hemispherical surface with symmetry property as a control surface, which could derivate a symmetric hybrid boundary integral equation easily to accomplish efficiently computation of floating body's hydrodynamics. The proposed method is applied to calculate the hydrodynamic coefficients of the hemispheres with analytical solutions, and good agreement is obtained when are compared with the hydrodynamic coefficients in the frequency domain. The results show that the proposed method has high accuracy in the calculation of hydrodynamic coefficients of floating bodies in time domain, and can save storage space and improve the calculation speed to a certain extent.

Keywords*: Time domain, Hybrid boundary method, Rankine source, Time domain Green function.*

I. INTRODUCTION

At present, Rankine source method and instantaneous time-domain Green function (TDGF) method are mainly used to calculate the hydrodynamic problems of ships and marine structures in time domain. Rankine source method in time domain can take into account the nonlinearity of free surface, nonlinearity of object surface and large motion of ship in hydrodynamic analysis[1,2]. The Green function of Rankine source method is simple and easy to calculate, but it needs to arrange the source and sink on the surface and the free surface of the object at the same time, and the numerical coast is generally adopted to meet its far-field radiation conditions[3]. The setting of remote radiation conditions often leads to the disadvantages of low accuracy, poor stability and large increase of free surface mesh number due to different experience of the calculators, which affects the mature application of Rankine source method. Although the calculation boundary of the TDGF method is only the wet surface of the ship, hundreds of millions of

Forest Chemicals Review
www.forestchemicalsreview.com
ISSN: 1520-0191
Sept-Oct 2021 Page No. 1243-1252
Article History: Received: 10 August 2021, Revised: 25 August 2021, Accepted: 05 September 2021, Publication: 31 October 2021

times are needed to call the TDGF and its partial derivative when the time-stepping method is applied to solve the velocity potential. The TDGF is an infinite integral, and the integrand function has the characteristics of high frequency oscillation and slow attenuation near the free surface. The numerical calculation of Green function and its partial derivative in time domain is very difficult, which affects the calculation efficiency, accuracy and stability. Meanwhile, this method is not suitable for the time domain hydrodynamic problems of the outward floating ship[4-6]. So a time-domain hybrid method which matching Rankine source method and TDGF method and providing a good treatment method for setting far-field radiation conditions of Rankine source method was developed by Wang[7], Hidetsugu [8], Dai and Duan[9], Tong[10], Shan[11] and so on.

When the above time-domain hybrid method is applied to the calculation, it is found that only the elements on the control surface still have the related calculation of TDGF. Therefore, in combination with the calculation of the symmetry of the floating body, this paper proposes to select the multi-degree-of-freedom symmetric geometric surface such as the hemispherical surface as the control surface, in order to improve the computational efficiency of the symmetric floating body hydrodynamic calculation.

II. ESTABLISHIMENT OF TIME DOMAIN MATCHED BOUNDARY INTEGRAL EQUATION

Establish Cartesian coordinate system as shown in Fig 1 that the *xoy* plane is on the still water surface, and the *z*-axis is vertically to the free surface. The control surface S_c divided the computational domain into internal domain Ω_I and external domain Ω_{II}. S_H is the body surface, S_F is the internal free surface, and the dotted line shows the initial state of calm water.

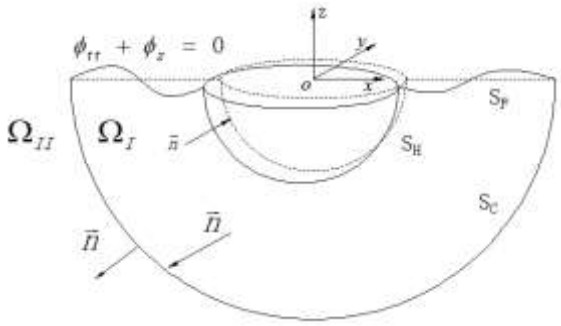

Fig 1: Cartesian coordinate system

When studying the interaction between ships and Marine structures and waves, it is considered that the fluid is a uniform, incompressible and non-viscous ideal fluid with no rotation flow, and the influence of lift force and surface tension is not taken into account.

Then the velocity potential at any point in the entire fluid domain can be expressed as:

Forest Chemicals Review
www.forestchemicalsreview.com
ISSN: 1520-0191
Sept-Oct 2021 Page No. 1243-1252
Article History: Received: 10 August 2021, Revised: 25 August 2021, Accepted: 05 September 2021, Publication: 31 October 2021

$$\begin{cases} \Phi^{I}(\vec{x};t) = \phi^{I}(\vec{x};t) + \phi_0(\vec{x};t); & \Omega_I \\ \Phi^{II}(\vec{x};t) = \phi^{II}(\vec{x};t) + \phi_0(\vec{x};t); & \Omega_{II} \end{cases} \tag{1}$$

Where, ϕ_o is the velocity potential of the incident wave with infinite water depth, and when approaching the wave, it is 180°, which can be expressed as:

$$\phi_0(x,y,z;t) = \frac{g\xi_a}{\omega}\exp(kz)\sin[k\varpi - \omega t] \tag{2}$$

Where, $\varpi = x\cos\beta + y\sin\beta$, and $k = \omega^2/g$ is wave number.

Considering the linear time domain radiation problem, the radiation velocity potential is:

$$\phi(\vec{x};t) = \sum_{k=1}^{6}\phi_k(\vec{x};t) \tag{3}$$

The radiation velocity potential is decomposed by the impulse response function method described by Cummins[12], and then the k mode velocity potential is decomposed into:

$$\phi_k(p,t) = \psi_k(p)\delta(t) + \chi_k(p,t) \tag{4}$$

$\psi_k(p)$ is the instantaneous velocity potential and $\chi_k(p,t)$ is the memory velocity potential respectively. They meet the following conditions:

$$\begin{cases} \nabla^2\psi_k = 0 & \\ \psi_k = 0 & ;on \quad S_F \\ \dfrac{\partial\psi_k}{\partial n} = n_k & ;on \quad S_H \end{cases} \tag{5}$$

$$\begin{cases} \nabla^2\chi_k = 0 & \\ \dfrac{\partial^2\chi_k}{\partial t^2} + g\dfrac{\partial\chi_k}{\partial z} = 0 & ;on \quad S_F \\ \dfrac{\partial\chi_k}{\partial n} = 0 & ;on \quad S_H \\ \chi_k\big|_{t=0} = 0 \ , \quad \dfrac{\partial\chi_k}{\partial t}\Big|_{t=0} = -g\dfrac{\partial\psi_k}{\partial z} & ;on \quad S_F \end{cases} \tag{6}$$

Then the velocity potential on control surface S_C, S_F and S_H satisfies the following integral equation separately:

$$\begin{cases} 2\pi\psi_k^I(p) + \iint_s \psi_k^I(q)\dfrac{\partial}{\partial n_q}\left(\dfrac{1}{r}\right)ds = \iint_s \dfrac{1}{r}\dfrac{\partial}{\partial n_q}\psi_k^I(q)ds \\ 2\pi\chi_k^I(p,t) + \iint_s \chi_k^I(q,t)\dfrac{\partial}{\partial n_q}\left(\dfrac{1}{r}\right)ds = \iint_s \dfrac{1}{r}\dfrac{\partial}{\partial n_q}\chi_k^I(q,t)ds \end{cases} \qquad (p,q\in S_C+S_F+S_H) \tag{7}$$

Forest Chemicals Review
www.forestchemicalsreview.com
ISSN: 1520-0191
Sept-Oct 2021 Page No. 1243-1252
Article History: Received: 10 August 2021, Revised: 25 August 2021, Accepted: 05 September 2021, Publication: 31 October 2021

$$\begin{cases} -2\pi\psi_k^{II}(p)+\iint_s \psi_k^{II}(q)\dfrac{\partial}{\partial n_q}\left(\dfrac{1}{r}-\dfrac{1}{r'}\right)ds=\iint_s\left(\dfrac{1}{r}-\dfrac{1}{r'}\right)\dfrac{\partial}{\partial n_q}\psi_k^{II}(q)ds \\ -2\pi\chi_k^{II}(p,t)+\iint_s \chi_k^{II}(q,t)\dfrac{\partial}{\partial n_q}\left(\dfrac{1}{r}-\dfrac{1}{r'}\right)ds=\iint_s\left(\dfrac{1}{r}-\dfrac{1}{r'}\right)\dfrac{\partial}{\partial n_q}\chi_k^{II}(q,t)ds \\ -\int_0^t d\tau\iint_s ds\left[\chi_k^{II}(q,t)\dfrac{\partial}{\partial n_q}G_f^{p,q}(t-\tau)-G_f^{p,q}(t-\tau)\dfrac{\partial}{\partial n_q}\chi_k^{II}(q,t)\right] \\ -\iint_s\left[\psi_k^{II}(q)\dfrac{\partial}{\partial n_q}G_f^{p,q}(t)-G_f^{p,q}(t)\dfrac{\partial}{\partial n_q}\psi_k^{II}(q)\right]ds \end{cases} \quad (p,q\in S_C) \tag{8}$$

$G_f^{p,q}(t)=2\int_0^\infty dk\sqrt{gk}\sin\left(\sqrt{gk}t\right)e^{kZ}J_0(kR)$ is the instantaneous TDGF proposed by Wehaus[13].

Then the velocity potential on control surface S_C shall meet the following requirements:

$$\begin{cases} \psi_k^I(p)=\psi_k^{II}(p) \quad , \quad \dfrac{\partial}{\partial n}\psi_k^I(p)=\dfrac{\partial}{\partial n}\psi_k^{II}(p) \\ \chi_k^I(p,t)=\chi_k^{II}(p,t) \quad , \quad \dfrac{\partial}{\partial n}\chi_k^I(p,t)=\dfrac{\partial}{\partial n}\chi_k^{II}(p,t) \end{cases} \tag{9}$$

III. NUMERICAL METHOD

The boundary integral equation satisfying the radiation problem is calculated by using the constant surface element method. In the discrete calculation, the boundary S_C, S_F and S_H are quadrilateral or triangular, and the number of surface elements is N_C, N_F and N_H. Introducing coefficient matrix:

$$A_{ij}=\begin{cases} 2\pi & , \quad i=j \\ \iint_{S_c+S_H+S_F} ds\dfrac{\partial}{\partial n_j}\left(\dfrac{1}{r_{ij}}\right) & , \quad i\neq j \end{cases} \tag{10-a}$$

$$\boldsymbol{B_{ij}}=\iint_{S_c+S_H+S_F}\boldsymbol{ds}\frac{\boldsymbol{1}}{\boldsymbol{r_{ij}}} \tag{10-b}$$

$$C_{ij}=\begin{cases} -2\pi-\iint_{S_c} ds\dfrac{\partial}{\partial n_j}\left(\dfrac{1}{r'_{ij}}\right) & , \quad i=j \\ \iint_{S_c} ds\dfrac{\partial}{\partial n_j}\left(\dfrac{1}{r_{ij}}-\dfrac{1}{r'_{ij}}\right) & , \quad i\neq j \end{cases} \tag{11-a}$$

$$\boldsymbol{D_{ij}}=\iint_{S_c}\boldsymbol{ds}\left(\frac{\boldsymbol{1}}{\boldsymbol{r_{ij}}}-\frac{\boldsymbol{1}}{\boldsymbol{r'_{ij}}}\right) \tag{11-b}$$

For the convenience of description, assume that the normal derivative of any variable $\Re$ is denoted as $\frac{\partial\Re}{\partial n}=\tilde{\Re}$. The angular mark k and coordinate point p and q are omitted for all the motion mode variables.

3.1 Solution of the Instantaneous Velocity Potential $\psi(p)$

Forest Chemicals Review
www.forestchemicalsreview.com
ISSN: 1520-0191
Sept-Oct 2021 Page No. 1243-1252
Article History: Received: 10 August 2021, Revised: 25 August 2021, Accepted: 05 September 2021, Publication: 31 October 2021

$\psi^{I}(p)$ and $\psi^{II}(p)$ satisfy the integral equation can be expressed by the coefficient matrix as,

$$[C]\{\psi_C^{II}\} = [D]\{\tilde{\psi}_C^{II}\} \tag{12}$$

$$[A]\left(\psi_C^I \quad \psi_H^I \quad \psi_F^I\right)^T = [B]\left(\tilde{\psi}_C^I \quad \tilde{\psi}_H^I \quad \tilde{\psi}_F^I\right)^T \tag{13}$$

According to Eq (12), $\{\psi_C^{II}\} = [C]^{-1}[D]\{\tilde{\psi}_C^{II}\}$. Substitute it into Eq (13), get:

$$\begin{bmatrix} A_{11} & A_{12} & A_{13} \\ A_{21} & A_{22} & A_{23} \\ A_{31} & A_{32} & A_{33} \end{bmatrix} \begin{Bmatrix} C^{-1}D\,\tilde{\psi}_C \\ \psi_F \\ \psi_H \end{Bmatrix} = \begin{bmatrix} B_{11} & B_{12} & B_{13} \\ B_{21} & B_{22} & B_{23} \\ B_{31} & B_{32} & B_{33} \end{bmatrix} \begin{Bmatrix} \tilde{\psi}_C \\ \tilde{\psi}_F \\ \tilde{\psi}_H \end{Bmatrix} \tag{14}$$

The numerical subscripts (1, 2, 3) of the coefficient matrix represent S_C, S_F and S_H respectively. Considering the continuous conditions on the control surface and the boundary conditions, the following equation can be obtained.

$$\begin{bmatrix} A_{11}C^{-1}D - B_{11} & -B_{12} & A_{13} \\ A_{21}C^{-1}D - B_{21} & -B_{22} & A_{23} \\ A_{31}C^{-1}D - B_{31} & -B_{32} & A_{33} \end{bmatrix} \begin{Bmatrix} \tilde{\psi}_C \\ \tilde{\psi}_F \\ \psi_H \end{Bmatrix} = \begin{bmatrix} B_{13} \\ B_{23} \\ B_{33} \end{bmatrix} \{\tilde{\psi}_H\} \tag{15}$$

And get,

$$[H]\begin{Bmatrix} \tilde{\psi}_C \\ \tilde{\psi}_F \\ \psi_H \end{Bmatrix} = [G_1]\{\tilde{\psi}_H\} \tag{16}$$

From the above equation, we can get: $\tilde{\psi}_C$, $\tilde{\psi}_F$ and ψ_H, and further get the initial value condition of memory velocity potential:

$$\frac{\partial \chi_F}{\partial t} = -g\tilde{\psi}_F, \quad t = 0 \tag{17}$$

3.2 Solution of the Memory Velocity Potential $\chi(p, t)$

Wang jianfang[7] proposed a free surface condition of integral form:

$$\chi_F(p,t) = -g\int_0^t d\tau(t-\tau)\frac{\partial \chi_F(p,\tau)}{\partial n} - gt\frac{\partial \psi_F(p)}{\partial n} \tag{18}$$

If the time interval is Δt, $M\Delta t$ and $m\Delta t$ represent the current moment and the historical moment respectively, then the discrete format of the internal free surface condition Eq (18) is:

$$\chi_j(M) = -g\cdot\Delta t^2\sum_{m=1}^{M-1}(M-m)\chi_j(m) - g\cdot M\cdot\Delta t\cdot\psi_j = -r_{Fj}(M)(j = 1,2,\cdots,N_F) \tag{19}$$

Introduction symbol:

$$r_{C1i}(M) = \sum_{m=1}^{M-1}\sum_{j=1}^{N_C}\left[\chi_j(m)\tilde{G}_f(M-m) - \tilde{\chi}_j(m)G_f(M-m)\right]\cdot\Delta t \tag{20}$$

$$r_{C2i}(M) = \sum_{j=1}^{N_C}\left[\psi_j\tilde{G}_f(M) - \tilde{\psi}_j G_f(M)\right] \tag{21}$$

Forest Chemicals Review
www.forestchemicalsreview.com
ISSN: 1520-0191
Sept-Oct 2021 Page No. 1243-1252
Article History: Received: 10 August 2021, Revised: 25 August 2021, Accepted: 05 September 2021, Publication: 31 October 2021

$$r_{Ci}(M) = r_{C1i}(M) + r_{C2i}(M) \quad (i=1,2,\ldots,N_C) \tag{22}$$

Then, the form of memory velocity potential matrix on the control surface S_C is

$$\{x_C\}^M = [C]^{-1}[D]\{\tilde{x}_C\}^M - [C]^{-1}\{r_C\}^M \tag{23}$$

The matrix of the memory velocity potential is obtained by considering the continuous conditions and boundary conditions on the control surface as well as the instantaneous velocity potential.

$$\begin{bmatrix} A_{11}C^{-1}D - B_{11} & -B_{12} & A_{13} \\ A_{21}C^{-1}D - B_{21} & -B_{22} & A_{23} \\ A_{31}C^{-1}D - B_{31} & -B_{32} & A_{33} \end{bmatrix} \begin{Bmatrix} \tilde{x}_C \\ \tilde{x}_F \\ x_H \end{Bmatrix} = \begin{bmatrix} A_{11}C^{-1} & A_{12} \\ A_{21}C^{-1} & A_{22} \\ A_{31}C^{-1} & A_{32} \end{bmatrix} \begin{Bmatrix} r_C \\ r_F \end{Bmatrix} \tag{24}$$

And get,

$$[H]\begin{Bmatrix} \tilde{x}_C \\ \tilde{x}_F \\ x_H \end{Bmatrix} = [G_2]\begin{Bmatrix} r_C \\ r_F \end{Bmatrix} \tag{25}$$

From the above equation, we can get: $\tilde{\chi}_C$, $\tilde{\chi}_F$ and χ_H, so far, the object velocity potential can be obtained through Eq (4).

3.3 Application of Symmetry in Time Domain Matching Method

Generally speaking, ships and marine structures have at least one symmetrical surface. For the convenience of description, this paper only considers the problem of *xoz* symmetry of control surface and object. Readers can refer to this method to extend to the control plane about *xoz* and *yoz* symmetry, object about *xoz* symmetry; and the control surface and object are symmetric about *xoz* and *yoz*.

Definition vector:

$$s_1 = (x-\xi, y-\eta, z-\zeta) \quad s_2 = (x-\xi, y-\eta, z+\zeta) \tag{26}$$

(x, y, z) and (ξ, η, ζ) in s_1, s_2 represent the coordinates of field point P and source point Q respectively.

Define Green function:

$$G(P,Q) = \frac{1}{r(P,Q)} - \frac{1}{r'(P,Q)} + G_f^{P,Q} = G_0 + G_1 + G_f \tag{27}$$

According to TDGF and G_1 expressions, geometric variables related to them can be represented by vector s_2, and G_0 are related to s_1.

Forest Chemicals Review
www.forestchemicalsreview.com
ISSN: 1520-0191
Sept-Oct 2021 Page No. 1243-1252
Article History: Received: 10 August 2021, Revised: 25 August 2021, Accepted: 05 September 2021, Publication: 31 October 2021

With reference to many symmetric studies, under the condition that the control surface is symmetric about *xoz*, the coefficient matrix C and D can express the submatrix form,

$$[C] = \begin{bmatrix} C_{11} & C_{14} \\ C_{14} & C_{11} \end{bmatrix}, \quad [D] = \begin{bmatrix} D_{11} & D_{14} \\ D_{14} & D_{11} \end{bmatrix} \tag{28}$$

Where, C_{11} is the influence coefficient matrix of the action of point Q on point P in its plane, and C_{14} is the influence coefficient matrix of Q′ on the effect of point P on the mirror image of point Q on the symmetry of xoz, as shown in Fig 2, matrix D is similar to it.

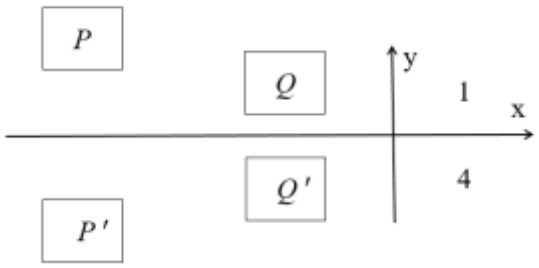

Fig 2: Sketch of symmetry description

$\tilde{\psi}_C^{II}$ is the normal derivative of the control surface, so when the motion mode k=1/3/5, $\tilde{\psi}_1^{II} = \tilde{\psi}_4^{II}$; When k=2/4/6, $\tilde{\psi}_1^{II} = -\tilde{\psi}_4^{II}$. Combining Eq (12) and Eq (28), it can be known that,

$$\begin{bmatrix} C_{11} & C_{14} \\ C_{14} & C_{11} \end{bmatrix} \begin{Bmatrix} \psi_1^{\mathrm{II}} \\ \psi_4^{\mathrm{II}} \end{Bmatrix} = \begin{bmatrix} D_{11} & D_{14} \\ D_{14} & D_{11} \end{bmatrix} \begin{Bmatrix} \tilde{\psi}_1^{\mathrm{II}} \\ (-1)^{k+1} \tilde{\psi}_1^{\mathrm{II}} \end{Bmatrix} \tag{29}$$

When *k*=1/3/5: $\left\{\psi_1^{\mathrm{II}}\right\} = \left[C_{11} + C_{14}\right]^{-1}\left[D_{11} + D_{14}\right]\left\{\tilde{\psi}_1^{\mathrm{II}}\right\} = \left\{\psi_4^{\mathrm{II}}\right\}$

When *k*=2/4/6: $\left\{\psi_1^{\mathrm{II}}\right\} = \left[C_{11} - C_{14}\right]^{-1}\left[D_{11} - D_{14}\right]\left\{\tilde{\psi}_1^{\mathrm{II}}\right\} = -\left\{\psi_4^{\mathrm{II}}\right\}$

For the convenience of description, the following only takes the vertical motion (k=3) as an example to illustrate, other modes as described or change the symbol in the corresponding position. Matrix is introduced, and the subscript 4/5/6 of the matrix represents the symmetric surface of control surface, free surface and object surface with respect to *xoz* symmetry, respectively.

$$[H_1] = \begin{bmatrix} A_{11}C^{-1}D - B_{11} & -B_{12} & A_{13} \\ A_{21}C^{-1}D - B_{21} & -B_{22} & A_{23} \\ A_{31}C^{-1}D - B_{31} & -B_{32} & A_{33} \end{bmatrix}, \quad [H_2] = \begin{bmatrix} A_{14}C^{-1}D - B_{14} & -B_{15} & A_{16} \\ A_{24}C^{-1}D - B_{24} & -B_{25} & A_{26} \\ A_{34}C^{-1}D - B_{34} & -B_{35} & A_{36} \end{bmatrix} \tag{30}$$

Forest Chemicals Review
www.forestchemicalsreview.com
ISSN: 1520-0191
Sept-Oct 2021 Page No. 1243-1252
Article History: Received: 10 August 2021, Revised: 25 August 2021, Accepted: 05 September 2021, Publication: 31 October 2021

$$[G_{11}]=\begin{bmatrix}B_{13}\\B_{23}\\B_{33}\end{bmatrix},\ [G_{12}]=\begin{bmatrix}B_{16}\\B_{26}\\B_{36}\end{bmatrix},\ \{X_1\}=\begin{Bmatrix}\tilde{\psi}_1\\\tilde{\psi}_2\\\psi_3\end{Bmatrix},\ \{X_2\}=\begin{Bmatrix}\tilde{\psi}_4\\\tilde{\psi}_5\\\psi_6\end{Bmatrix},\ \{N_1\}=\{\tilde{\psi}_1\},\{N_2\}=\{\tilde{\psi}_4\}$$

When *k*=3, Eq (16) can be expressed,

$$\begin{bmatrix}H_1 & H_2\\H_2 & H_1\end{bmatrix}\begin{Bmatrix}X_1\\X_2\end{Bmatrix}=\begin{bmatrix}G_{11} & G_{12}\\G_{12} & G_{11}\end{bmatrix}\begin{Bmatrix}N_1\\N_1\end{Bmatrix},\ \{X_1\}=\begin{Bmatrix}\tilde{\psi}_1\\\tilde{\psi}_2\\\psi_3\end{Bmatrix}=[H_1+H_2]^{-1}[G_{11}+G_{12}]\{N_1\} \quad (31)$$

At this point, the instantaneous velocity potential on the surface is obtained through symmetry:

$$\{\psi_3\}=\{\psi_6\} \quad (32)$$

Similarly, the memory velocity potential on the object surface can be obtained by Eq (25):

$$\{\chi_3\}=\{\chi_6\} \quad (33)$$

After obtaining the instantaneous velocity potential and memory velocity potential on the surface of the object, the time domain hydrodynamic force, impulse memory function, additional mass and damping coefficient of the floating body can be calculated through Liapis.

IV. NUMERICAL RESULTS AND ANALYSIS

In this paper, hemispheres with radius r=1m were selected to calculate floating bodies, and the calculated control surface radius was 5m, as shown in Fig 3, in which the control surface mesh number was 300, the free surface mesh number was 400, and the object surface mesh number was 260. In order to compare with the analytical results provided by Barakat[14], this paper only takes the vertical additional mass, damping coefficient and delay function as examples, as shown in Fig 4 and Fig 5.

Fig 4 is the dimensionless memory impulse response function curve of hemisphere, Fig 5 is the dimensionless joint curve of additional mass and damping coefficient. Fig 4 and Fig 5 reflect the instantaneous motion problem (radiation problem) of three-dimensional floating body in the time domain.

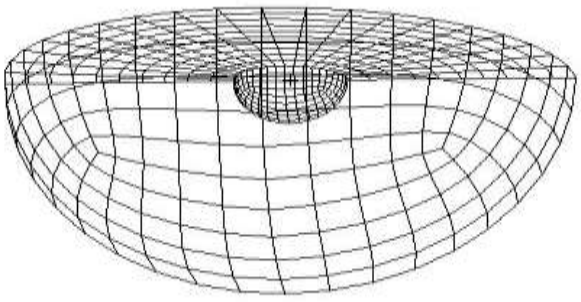

Forest Chemicals Review
www.forestchemicalsreview.com
ISSN: 1520-0191
Sept-Oct 2021 Page No. 1243-1252
Article History: Received: 10 August 2021, Revised: 25 August 2021, Accepted: 05 September 2021, Publication: 31 October 2021

Fig 3: Grid of hemisphere

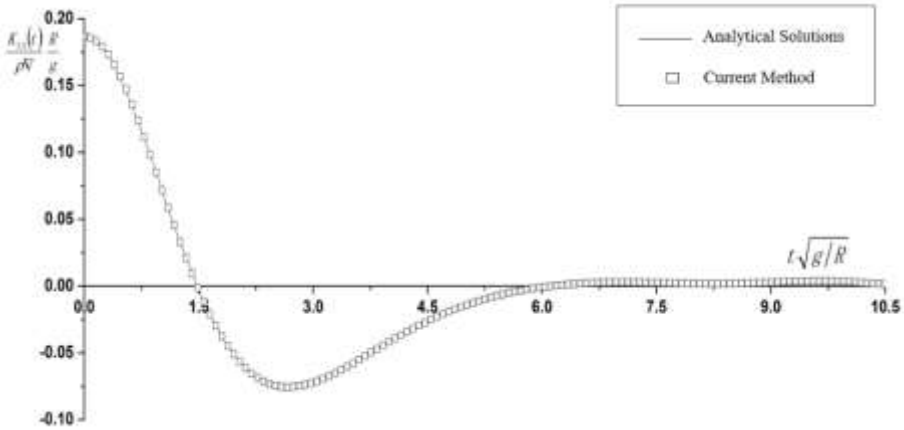

Fig 4: Nondimensional memory impulsive response function K33

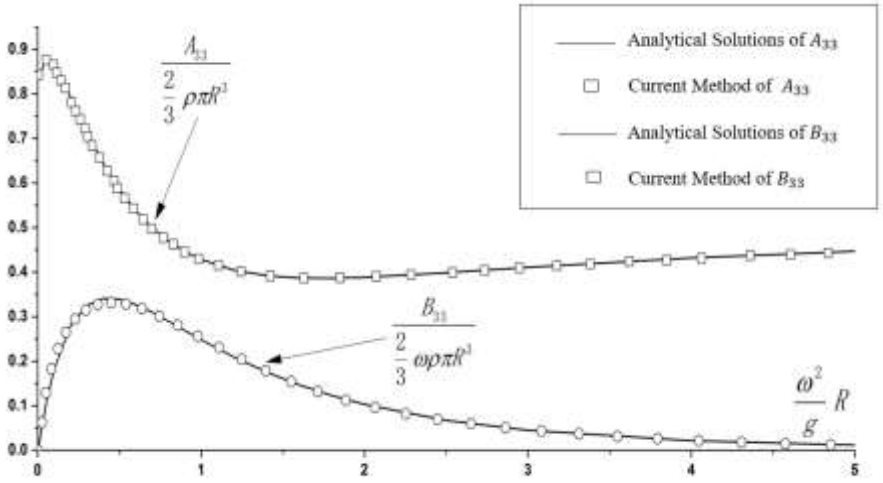

Fig 5: Nondimensional hydrodynamic coefficient

The results above verify the correctness and effectiveness of the proposed method. The numerical treatment method described in this paper is applicable to conventional ships with plane symmetry of xoz, and it is not difficult for readers to extend it to Marine structures with symmetry of xoz and yoz, such as floating platforms. At the same time, only the control surface contains the relevant numerical calculation of TDGF, so the characteristics of the semi-sphere about angular axisymmetric can be considered. These works will certainly improve the numerical calculation efficiency of floating body motion and wave force in the time domain, which is of great significance for the engineering application of this direction.

Forest Chemicals Review
www.forestchemicalsreview.com
ISSN: 1520-0191
Sept-Oct 2021 Page No. 1243-1252
Article History: Received: 10 August 2021, Revised: 25 August 2021, Accepted: 05 September 2021, Publication: 31 October 2021

V. CONCLUTION

The hybrid method of Rankine source method and the TDGF method inherits the advantages of Rankine source method and also solves Rankine far-field radiation condition which is difficult to be satisfied by source method. The method proposed in this paper focuses on how to calculate accurately and quickly the TDGF on the control surface of symmetric floating body and the numerical treatment of the integral equation it satisfies. Compared with the analytical solution, it can be seen that the proposed method can effectively realize the time-domain calculation of ships, and is easy to operate, which provides a basis for the rapid calculation of ship with forward speed problems.

ACKNOWLEDGEMENTS

This research was supported by National Natural Science Foundation of China (Grant No. 51909155), Shanghai High-level Local University Innovation Team (Maritime safety & technical support).

REFERENCES

[1] KIM Y, KIM K H, KIM J H, et al (2013). Time-domain analysis of nonlinear motion responses and structural loads on ships and offshore structures: development of WISH programs. International Journal of Naval Architecture and Ocean Engineering 3:37-52.
[2] HE G, KASHIWAGI M (2014). A time-domain higher-order boundary element method for 3D forward-speed radiation and diffraction problems. Journal of Marine Science and Technology 19:228-244.
[3] Nakos D E, Sclavounos P D (1990). On Steady and Unsteady Ship Wave Patterns. Journal of Fluid Mechanics 215:263-288.
[4] BECK R F, LIAPIS S J (1987). Transient motions of floating bodies at zero forward speed. Journal of Ship Research 31:164-176.
[5] CLEMENT A H (1998). An ordinary differential equation for the Green function of time-domain free-surface hydrodynamics. Journal of Engineering Mathematics 33:201-217.
[6] ZHU R, ZHU H, SHEN L, et al (2007). Numerical treatments and applications of the 3D transient green function. China Ocean Engineering 21:637-646.
[7] Wang J F. Numerical Simulation of the Linear Free Surface Condition. Dissertation. Ship and Marine structure design and manufacturing specialty. Harbin Engineering University, Harbin, 2002.
[8] Shiro KATAOKA, Hidetsugu IWASHITA, et al (2004). A time-domain hybrid method for calculating the wave source of seakeeping. The Japan Society of Naval Architects and Ocean Engineers 108:61-72.
[9] Dai yishan, Duan wenyang (2008). Potential Flow Theory of Ship Motions in Waves. National Defense Industry Press.
[10] Tong Xiaowang, Li Hui, Ren Huilong (2013). A hybrid approach applied to fast calculating the time-domain ship motions. Journal of Ship Mechanics 17:756-762.
[11] Shan P, Wang Y, Wang F, Wu J, Zhu R (2020). Froude-Krylov nonlinear computations of three dimensional wave loads by a hybrid time domain boundary element method. Ocean Engineering, 2020, 195.
[12] Cummins W E (1962). The Impulse Response Function and Ship Motions. Schiffstechnik 9:101-109.
[13] Wehause J V , Laitone E V (1960). Surface Waves. SpringVerlag.
[14] Barakat R (1962). Vertical motion of a floating sphere in a sine-wave sea. Journal of Fluid Mechanics 13:540-556.